ACS APPLIED MATERIALS & INTERFACES

Research Article

www.acsami.org

Hierarchically Ordered Self-Lubricating Superhydrophobic Anodized Aluminum Surfaces with Enhanced Corrosion Resistance

Panneerselvam Vengatesh and Manickam Anbu Kulandainathan*

Electro-Organic, CSIR-Central Electrochemical Research Institute, Karaikudi 630 006, India

Supporting Information

ABSTRACT: Herein, we report a facile method for the fabrication of self-lubricating superhydrophobic hierarchical anodic aluminum oxide (AAO) surfaces with improved corrosion protection, which is greatly anticipated to have a high impact in catalysis, aerospace, and the shipping industries. This method involves chemical grafting of as-formed AAO using low surface free energy molecules like long chain saturated fatty acids, perfluorinated fatty acid (perfluorooctadecanoic acid, PFODA), and perfluorosulfonicacid-polytetrafluoroethylene copolymer. The pre and post treatment processes in the anodization of aluminum (Al) play a vital role in the grafting of fatty acids. Wettability and surface free energy were analyzed using a contact angle meter and achieved 161.5° for PFODA grafted anodized aluminum (PFODA-Al). This study was also aimed at evaluating the surface for corrosion resistance by Tafel polarization and self-lubricating properties by tribological studies using a pin-on-disc tribometer. The collective results showed that chemically grafted AAO nanostructures exhibit high corrosion resistance toward seawater and low frictional coefficient due to low surface energy and self-lubricating property of fatty acids covalently linked to anodized Al surfaces.

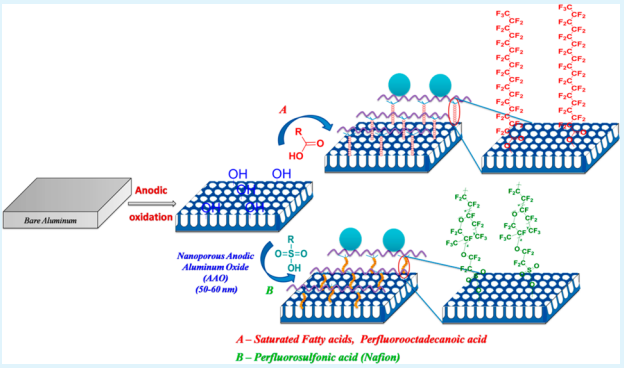

KEYWORDS: *nanoporous anodic aluminum oxide, perfluorooctadecanoic acid, superhydrophobic, corrosion protection, frictional coefficient*

1. INTRODUCTION

Aluminum (Al) and its alloys are naturally abundant engineering materials with extensive applications in daily life, which include aerospace, shipping industries, transportation, packaging, construction, and household items because of their high strength, excellent heat and electrical conductivities, and low weight. In recent years, nanoporous anodic aluminum oxide (AAO) prepared by the electrochemical anodization of Al[1] have attracted significant attention for their potential application prospects in engineering technologies. This profound interest led researchers to achieve highly ordered AAO for multifarious applications, which include catalysis,[2] drug delivery,[3,4] biosensing,[5−7] template synthesis,[8−10] molecular and ion separation,[11−13] and so-forth.

By using an appropriate acidic electrolyte,[14] it is possible to achieve nanopores with controlled pore size. Apart from this, the anodization parameters such as temperature, current, pH, applied potential, electrolyte concentration, and pre-patterning of the surface should also be taken into account in order to achieve highly ordered pore structures with desired and tunable pore diameters and interpore distance.[15] Numerous studies have revealed the mechanism for the formation of AAO. Recently, Reis et al.[16] proposed a model for the growth of nanoporous AAO by anodic oxidation. Ngan et al.[17] also investigated the sustainable growth of nanopore channels in AAO guided with pre-patterns by focused ion-beam milling. In general, the formation of AAO on the Al surface could act as a corrosion barrier, but it was limited to a certain extent due to its hydrophilic nature. Therefore, it is quite necessary to modify Al surfaces with enhanced hydrophobicity (so-called superhydrophobicity) for improved corrosion resistance.[18−21]

Superhydrophobic surfaces are characterized by three main properties; high water contact angle (WCA > 150°), low sliding angle (SA < 5°), and very low contact angle hysteresis (CAH < 5°).[22] These characteristics gives rise to certain applicative properties, such as self-cleaning, anti-icing, antifouling, corrosion resistance, fluidic drag reduction, and oil/water separation.[23−28] In order to make a substrate superhydrophobic, it is necessary to increase the surface roughness and lower the surface free energy. In this scenario, numerous methods have been developed to fabricate superhydrophobic surfaces, which include etching techniques,[24,29] the sol−gel process[30,31] electrospinning,[32] deposition of nanoparticles on smooth or rough substrates,[33] the LbL technique,[34,35] chemical bath deposition (CBD),[36] physical vapor deposition (PVD),[37] and the solution-immersion process,[38] owing to their wide range of

Received: September 24, 2014
Accepted: December 22, 2014
Published: December 22, 2014

DOI: 10.1021/am506568v
ACS Appl. Mater. Interfaces 2015, 7, 1516−1526

applications in emerging trends. Among these methods, the solution immersion process is an effective yet quicker process with the potential to be used on various substrates. Recent research has focused on preparing superhydrophobic surfaces with higher corrosion and wear resistance by creating micro/nano scale (dual scale) roughness and subsequent modification with low surface energy molecules.[39−42]

Long chain fatty acids are used as effective modifiers since they possess low surface energy and are chemisorbed onto the substrate forming stable carboxylate groups.[43,44] For instance, dodecanoic acid (lauric acid) modified Al alloy, as shown by Wen et al.,[24] demonstrates an excellent anti-icing behavior. Recently Feng et al.[45] also developed a novel superhydrophobic alumina surface with a contact angle of 154.2° by grafting an octadecanoic (stearic acid) layer onto the porous and roughened Al film. Apart from these fluorine-containing chemicals like fluoroalkylsilanes[38,46,47] and fluoropolymers,[48] polymers[49] have also been utilized for the fabrication of superhydrophobic alumina surfaces because of their low surface energy. More recently, Chin et al.[50] developed liquid marbles using TiO_2 nanoparticles encapsulated with perfluorooctadecanoic acid, which shows an excellent photo-responsive behavior. Fatty acids and perfluorinated fatty acids are found to have self-lubricating properties in addition to their superhydrophobic behavior, which helps to minimize the friction and wear and serves as a barrier for corrosion protection.[51−53] These molecules possess good lubricity and are commonly used in hard disc drives and in the electronic industry as high performance nanolubricants.

Increasing the durability, corrosion, and wear resistance of the final products and simplifying the fabrication process are the few concerns that need to be resolved for large-scale manufacturing of superhydrophobic surfaces. In view of this, we developed a nanopore embedded microtextured superhydrophobic Al surface with a low frictional coefficient and high resistivity to corrosion by combining two processes, viz., electrochemical anodization followed by a grafting process utilizing long chain saturated fatty acids, perfluorinated fatty acid, or perfluorinated sulfonic acid. We also studied the effect of increasing roughness on the superhydrophobicity of the developed surface with an increase in the number of carbon atoms of the long chain fatty acids. The durability of as-prepared samples were tested and compared with freshly prepared samples. The corrosion resistance of the grafted as well as the anodized Al surfaces was studied using the Tafel polarization technique. Friction reducing behavior and antiwear properties were also investigated via a dry tribology study and compared with that of the bare substrate.

2. EXPERIMENTAL SECTION

2.1. Materials. Aluminum plates [(6.35 mm) thick, 99.95% (metal basis)], perfluorooctadecanoic acid (PFODA) and perfluorosulfonic acid-PTFE copolymer (Nafion, PFSA) were obtained from Alfa Aesar, India. Dodecanoic acid (DDA), tetradecanoic acid (TDA), octadecanoic acid (ODA), and icosanoic acid (ISA) were purchased from Sigma-Aldrich (India). All other reagents were of analytical grade and were used without further purification. Deionized water (DI) with a resistivity of 18.2 MΩ cm was used in all the experiments.

2.2. Modification of Al Surfaces. *2.2.1. Procedure to Prepare Electropolished Al Surface.* The Al plates were annealed in a conventional vacuum furnace at 250 °C for 2 h, followed by mechanical polishing with SiC papers of different grid sizes (400 and 40) and cut into pieces of size 1.5 × 5.0 cm^2. The pieces were cleaned ultrasonically in the sequence of alcohols and DI for 5 min, respectively, and dried at 100 °C. The cleaned and dried Al pieces were then electropolished[54] in 1:4 $HClO_4$/EtOH at 25 °C (10 V for 2 min).

2.2.2. Procedure for the Preparation of Anodic Aluminum Oxide (AAO) Surface. Nanoporous AAO preparation was performed in an electrochemical cell with a conventional two-electrode configuration consisting of a platinum sheet as the counter electrode and electropolished Al substrates as the working electrode. One-step anodic oxidation was carried out. Briefly, Al sheets were anodized in 0.3 M oxalic acid at a constant voltage of 30 V for 3 h at 25 °C. After anodization, the samples were dipped in a 5% H_3PO_4 solution at 35 °C for 10 min to allow the nanoporous opening. However, microvalleys were created on the electropolished Al surfaces when sulfuric acid was used as an electrolyte, and the detailed procedure is provided as Supporting Information (SI) S1.

2.2.3. Procedure for Grafting of Organic Molecules onto AAO Surface. Anodized Al plates were immersed into the solution containing saturated fatty acids (1 wt % in EtOH) for 5 min and dried in an oven at 110 °C for 1 h. 0.1 wt % of PFODA solution in EtOH was also prepared, and the plates were immersed into this solution for 10 s and then dried as mentioned above. Similarly, 0.1 wt % of PFSA in 1:1 H_2O/EtOH solution have also been prepared and grafted on anodized Al.

2.3. Characterization. FTIR spectra were recorded on Attenuated Total Reflection (ATR) mode using BRUKER-TENSOR 27 (Optik GmbH) equipped with RTDLaTGS (Varian) detector. All analyses were performed in the range of 400−4000 cm^{-1}, with a resolution of 4 cm^{-1} after 64 scans. Nanoporous AAO was used as the reference. The spectra of fatty acids were taken by pressed pellet technique using KBr. The morphological structures of the prepared samples were captured using Scanning Electron Microscopy (SEM) of TESCAN, VEGA 3 fitted with Bruker detector, Czeck Republic. Field Emission Scanning Electron Microscopy (FESEM, Carl Ziess Model no. SUPRA 55VP) was also used to acquire the surface morphology of the nanostructured anodized and grafted Al surfaces. Gold was sputtered onto the samples before analyzing the morphology in order to increase the conductivity. The roughness and surface topography of the bare and treated samples were obtained using AFM from Agilent Technologies, U.S.A.; Model No. 5500 with Si_3N_4 cantilever. AFM images were taken in tapping mode with a scan area of 2 × 2 μm^2. The profile extractions of the topographical images were done by using Picoview 1.12.2 software.

The chemical compositions of modified samples were analyzed using X-ray photoelectron spectroscopy technique (Multilab 2000, Thermoscientific, U.K). Spectra were recorded using an X-ray source of Al Kα radiation with a scan range of 0−1200 eV binding energy and referenced with respect to adventitious carbon (C 1s: 284.9 eV). The chamber pressure was about 3 × 10^{-8} Torr, and the pass energy was 20 eV under testing conditions. The collected high-resolution XPS spectra were fitted according to the Shirley-type background using XPS PEAK 4.1 software programmed with Gaussian-Lorentzien 60%/40%. The EDX spectra (Thermo Electron Corporation, U.S.A.) were acquired at an accelerating voltage of 20.0 kV and a magnification of 1000×. The wettability of bare and treated samples was measured on Automatic Video based Contact angle measuring instrument from Data Physics Instruments GmbH (Model OCA 35), Germany, by means of water contact angle and CAH at ambient and high temperature. The analyses were carried out using the sessile drop method for static and dynamic contact angles and sessile drop (needle in) method for advancing and receding contact angles, respectively. The tilting angle was calculated with respect to the pendant drop method. Water droplets of 5 μL were used for all the measurements.

2.4. Electrochemical Studies. Corrosion parameters were measured through Tafel polarization technique using BAS-IM6, U.S.A. electrochemical workstation in a three-electrode system: Al plate (1 cm^2) as a working electrode, a platinum gauze counter electrode, and a saturated calomel electrode as a reference electrode. After keeping the electrode ideal for a stable open circuit potential (OCP) for 30 min in an electrolyte containing 3.5 wt % NaCl solution, the potentiodynamic polarization curves were acquired at a scan rate of 1 mV/s at room temperature for bare, AAO, and modified Al surfaces.

DOI: 10.1021/am506568v
ACS Appl. Mater. Interfaces 2015, 7, 1516−1526

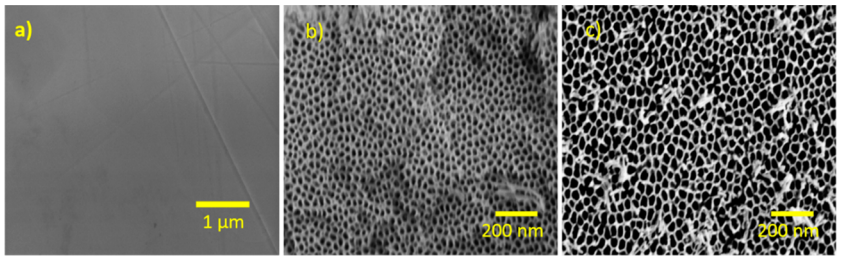

Figure 1. FESEM images of (a) bare (electropolished Al), (b) nanoporous anodic aluminum oxide (AAO) obtained from the anodization of electropolished Al using oxalic acid as electrolyte (before etching), and (c) after etching with phosphoric acid for 10 min.

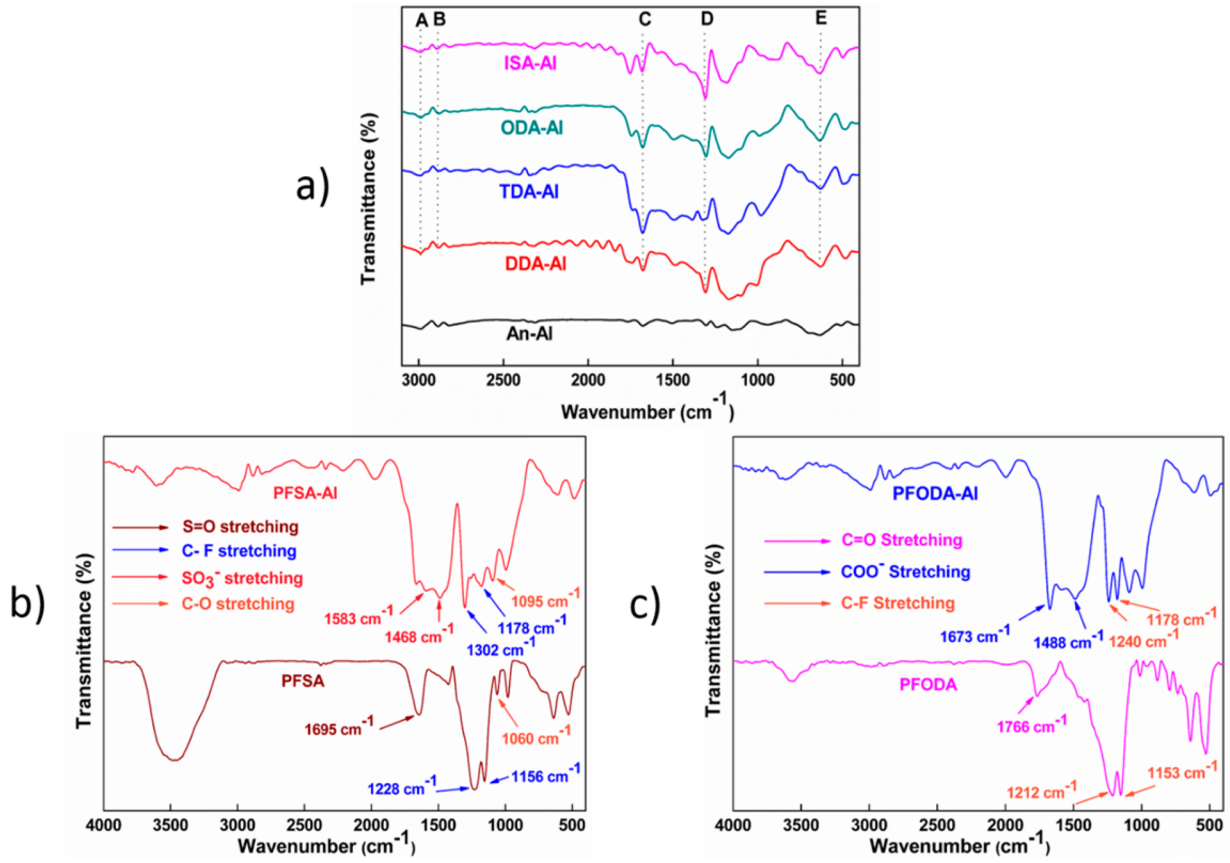

Figure 2. (a) FTIR spectrum of An-Al, DDA-Al, TDA-Al, ODA-Al, and ISA-Al recorded in ATR mode, (b) and (c) FTIR spectra of PFSA-Al, PFODA-Al recorded in ATR mode and PFSA, PFODA recorded using KBr Pellet technique. The regions A to E in (a) is explained in detail in the text.

Immersion tests were also carried out with 3.5 wt % NaCl solution to evaluate the durability of modified Al surfaces. After a definite time of immersion, the samples were taken out from the water and dried in a vacuum oven at 40 °C for 5 min. Then, the wettability of the samples was evaluated by the aforementioned method.

2.5. Tribological Studies. Dry tribology properties have been investigated using pin-on-disc type tribometer from Nanotech Systems (Model No. TR-20LE-PHM 400-CHM 500), India. The sliding distance was kept constant for all the samples as 60 mm and tested for 10 000 cycles against stainless steel SS 301 disc. The above studies were performed at an applied load of 10 N to evaluate the self-lubricative property of the modified substrates. The friction coefficient obtained from the instrument was plotted against sliding cycles.

3. RESULTS AND DISCUSSION

3.1. Formation of Nanopores. Uniform roughness was created on the pretreated (electropolished) Al surface by one-step anodic oxidation process. In particular, the pretreated Al samples were subjected to anodization under mild conditions, which is denoted as a mild anodization (MA) process, in which constant voltage was supplied for the oxidation of Al to AAO. To evaluate the surface features of the anodized aluminum surface, FESEM images are provided as Figure 1. In this process, ordered uniform nanopores with pore sizes ~40 nm were formed using oxalic acid (30 V, 25 °C, 3 h) which could be clearly seen in Figure 1b, whereas the FESEM image of the electropolished featureless Al surface can be seen in Figure 1a. The dimension of pores and pore structures can be tuned by altering the acidic nature of the electrolyte, and applied voltage.[14]

After anodization, wet chemical etching was carried out with the help of phosphoric acid, which allows pore widening to take place that can be clearly visualized from the FESEM image shown in Figure 1c. The size of the nanopores was around 30–40 nm before etching, and it was found to be 50–60 nm after

DOI: 10.1021/am506568v
ACS Appl. Mater. Interfaces 2015, 7, 1516–1526

etching, and they were consistently distributed throughout the surface. It is also found that the modification (covalent bond formation) was easier and effective with the postetched surfaces having larger pore diameters when compared to surfaces having smaller pore diameters. This is mainly because of widening of the pores by wet chemical etching.[47] Hence, an appropriate pore size of the nanopores was taken into account in order to attain efficient chemical modification on AAO surfaces.

In an attempt to get nanopores embedded with microtexture with increased surface roughness, acid etching was done at the electropolished Al surfaces followed by anodization in the presence of sulfuric acid electrolyte.[39] As a result, we could get microvalleys in the range of 2.1 μm in height (SEM image presented as Figure S1 in the SI). Although the roughness was increasing (analyzed by AFM), the modification was found to be ineffective toward fatty acids. This ineffectiveness was attributed to the smaller pore size and insufficient hydroxyl groups on the surface, which is evident from its wettability. Hence the anodization was done using oxalic acid for all the experiments. It is also noted that the ease of grafting, in the case of nanoporous AAO with desired pore diameters, is considerably higher for fatty acids, perfluoro fatty acids, and perfluoro sulfonic acids (particularly PFODA and nafion) as compared to the etched surfaces.

3.2. Surface Modification. Saturated fatty acids from DDA (12 C) to ISA (20 C), perfluorinated carboxylic acid (PFODA) or perfluorinated sulfonic acid (Nafion, PFSA) are the low surface energy modifiers used in the present study for modifying the anodized Al surface. FTIR-ATR spectra of anodized Al using oxalic acid (An-Al) and chemically modified Al are shown in Figure 2. Saturated fatty acids modified An-Al was indicated by DDA-Al, TDA-Al, ODA-Al, and ISA-Al, depending on their increase in the number of carbon atoms. FTIR-ATR spectra of saturated fatty acids are also acquired in order to compare them with functionalized substrates (provided in the SI as Figure S2). Figure 2a shows the FTIR spectra of An-Al and the corresponding saturated fatty acids functionalized An-Al. The peaks around the region A (2990 cm^{-1}) and region B (2886 cm^{-1}) was assigned to asymmetric (υ_{as}) and symmetric (υ_s) stretching vibrations of methylene group. In addition to this, there are peaks present at 2958 and 2896 cm^{-1} which are attributed to the υ_{as} and υ_s of methyl groups situated at head region, respectively. These vibrational modes are mainly corresponding to the alkyl chains of fatty acids. The formation of stable carboxylate groups which were bound to the Al surface was confirmed by the presence of υ_s and υ_{as} of CO_2^- at the region of C (1681 cm^{-1}) and D (1308 cm^{-1}), respectively.[38] The region E (638 cm^{-1}) was responsible for the CH_2 in-plane bending vibrations. We have noticed the increase in the frequency of CH_2 in-plane bending vibrations from 625 to 638 cm^{-1} which is due to an increase in the number of CH_2 groups, and it is observed that the same peak was shifted from their corresponding fatty acids (548 to 560 cm^{-1}) before modifying with AAO, which provides an additional information about chemical modification.

Figure 2b,c shows the FTIR spectra of An-Al, PFSA modified An-Al (PFSA-Al) and PFODA modified An-Al (PFODA-Al). C−F stretching vibrations are clearly shown by the peaks at 1302, 1178 cm^{-1} (PFSA-Al) and 1240, 1178 cm^{-1} (PFODA-Al), which is shifted from the parent 1228, 1156 cm^{-1} (PFSA) and 1212, 1153 cm^{-1} (PFODA), respectively. The formation of sulfonates from PFSA were confirmed by the peaks present at 1583 and 1468 cm^{-1} in Figure 2b which was assigned to SO_3 stretching vibrations. The peaks at 1673 and 1488 cm^{-1} in Figure 2c represents υ_{as} and υ_s of —O—C═O, as described in the saturated fatty acids modified An-Al, confirms the formation of stable carboxylate groups with An-Al. These collective results obtained from FTIR-ATR spectra clearly reveal the formation of carboxylates and sulfonates from their respective acids on the An-Al surface.

3.3. Surface Morphological Studies. SEM and AFM techniques were used to observe the surface morphology of AAO and chemically grafted AAO samples. Saturated fatty acids such as DDA, TDA, ODA and ISA, PFODA, and PFSA were used to fabricate the as-formed nanopores. These organic molecules are being introduced particularly to impart superhydrophobicity, corrosion resistive, and wear resistive properties. Figure 3 shows SEM images of saturated fatty acids

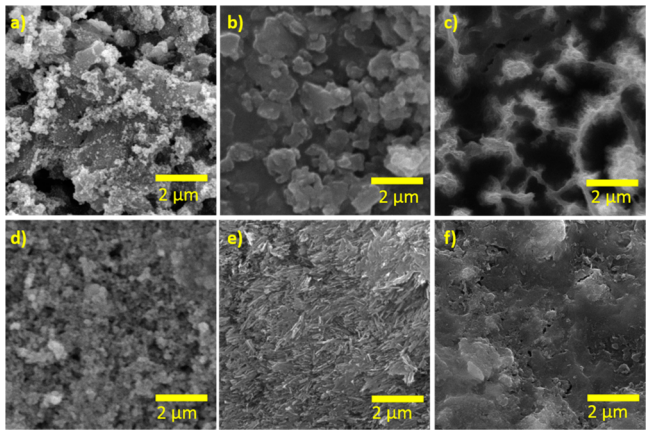

Figure 3. SEM images showing micro and nanotextured surfaces of (a) DDA-Al, (b) TDA-Al, (c) ODA-Al, (d) ISA-Al, (e) PFODA-Al, and (f) PFSA-Al.

(number of carbon atoms from 12 to 20 C), PFODA and PFSA modified An-Al surfaces. We compared the morphology of smooth bare Al surface with that of the rough An-Al surface and the chemically modified An-Al surface to understand the ordered homogeneous hierarchical roughness. The morphological changes in micro and nanostructured substrates are clearly depicted in Figure 3a−f. It is possible to observe the formation of dual-scale roughness on modified An-Al with microbunches (DDA-Al, TDA-Al), microbranch-like structure (ODA-Al), microsponges (ISA-Al), micro/nanosticks (PFODA-Al), and uniform layer like structure (PFSA-Al). It is also noted that the as-formed nanopores on An-Al surfaces are being completely filled by the organic molecules utilized for grafting, which led to microtextured surfaces. So the superhydrophobic behavior was attained due to these hierarchically aligned surfaces in addition to the low surface energy, as discussed later. A branch-like structure is formed when PFODA was coated onto as-formed microvalleys using sulfuric acid, which is indicated by the SEM images (provided as Figure S1 in the SI).

AFM technique, a well-established tool, is used to observe the changes in the surface topography and roughness of various metal substrates before and after modification. Figure 4 illustrates the surface topography of bare, An-Al, PFSA-Al, and PFODA-Al. The rms roughness (R_{rms}) was found to be 0.156 nm (bare), 15.0 nm (An-Al), 24.0 nm (PFSA-Al) and 36.7 nm (PFODA-Al).[55] It is evident that the roughness of treated substrates increases from bare Al to An-Al and in turn

DOI: 10.1021/am506568v
ACS Appl. Mater. Interfaces 2015, 7, 1516−1526

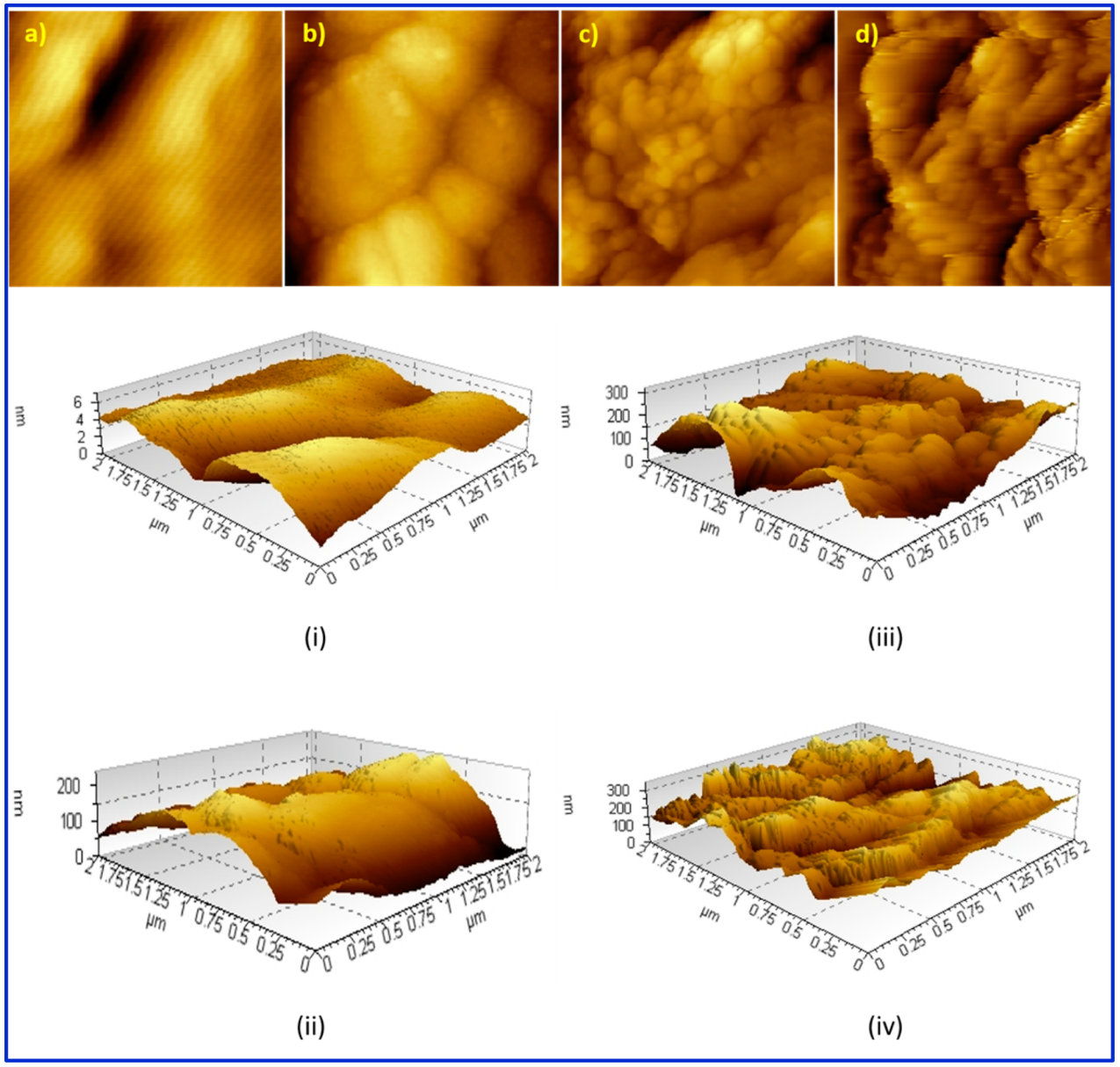

Figure 4. AFM tapping mode topographical images and 3D images of Bare (a) and (i), An-Al (b) and (ii), PFSA-Al (c) and (iii), and PFODA-Al (d) and (iv). 3D images clearly show the formation of hierarchical roughness. The roughness parameters were obtained by profile extraction of topographical images. Scan area 2 × 2 μm^2.

to chemically modified An-Al. Interestingly, AFM images revealed that the terraces of oxide nanostructures were significantly enlarged after grafting with organic molecules. AFM 3D images also provide more direct evidence on the nanostructures of AAO and modified Al surfaces, which is outlined in Figure 4(i–iv). AFM tapping mode 3D images of saturated fatty acids modified An-Al and the corresponding topographical images are reported to exemplify the roughness (Figure S3 in the SI). In addition to FTIR-ATR spectral data, the surface morphological studies using the above instrumental techniques clearly demonstrate the changes occurred on the surface of Al before and after treatments.

3.4. Surface Elemental Composition. The surface elemental compositions of fabricated samples were analyzed using EDX spectroscopy and X-ray photon electron spectroscopy (XPS) techniques. The EDX spectrum of An-Al shows Al and O in atomic % of 36 and 62, respectively (see Figure S5a given in the SI), which confirms the formation of nanoporous AAO with hydroxyl groups on the surface. After being modified with PFODA, PFSA, and fatty acids, corresponding EDX spectra were also acquired to find the elements present on the surface (see SI S5b-d). In addition to EDX spectroscopy, XPS spectroscopy was also utilized to confirm the aforementioned changes on the surface. This spectroscopy was one of the surface sensitive techniques used to provide information on the changes in surface chemistry. XPS survey scan spectra of ISA-Al (SI Figure S6a) consisted of three elements: Al, C, and O. In addition to these elements, F was also seen in the survey scan spectra of PFODA-Al provided in SI Figure S6b. Figure 5 shows the deconvoluted spectra of ISA-Al which indicates the following elements; Al 2p (75.1 eV), Al 2s (120.2 eV), C 1s (285 eV), and O 1s (531 eV), respectively. It should be noted that the spectra of C 1s contains four peaks. The first peak at 284.2 eV was attributed to —C—H group and the second peak

DOI: 10.1021/am506568v
ACS Appl. Mater. Interfaces 2015, 7, 1516–1526

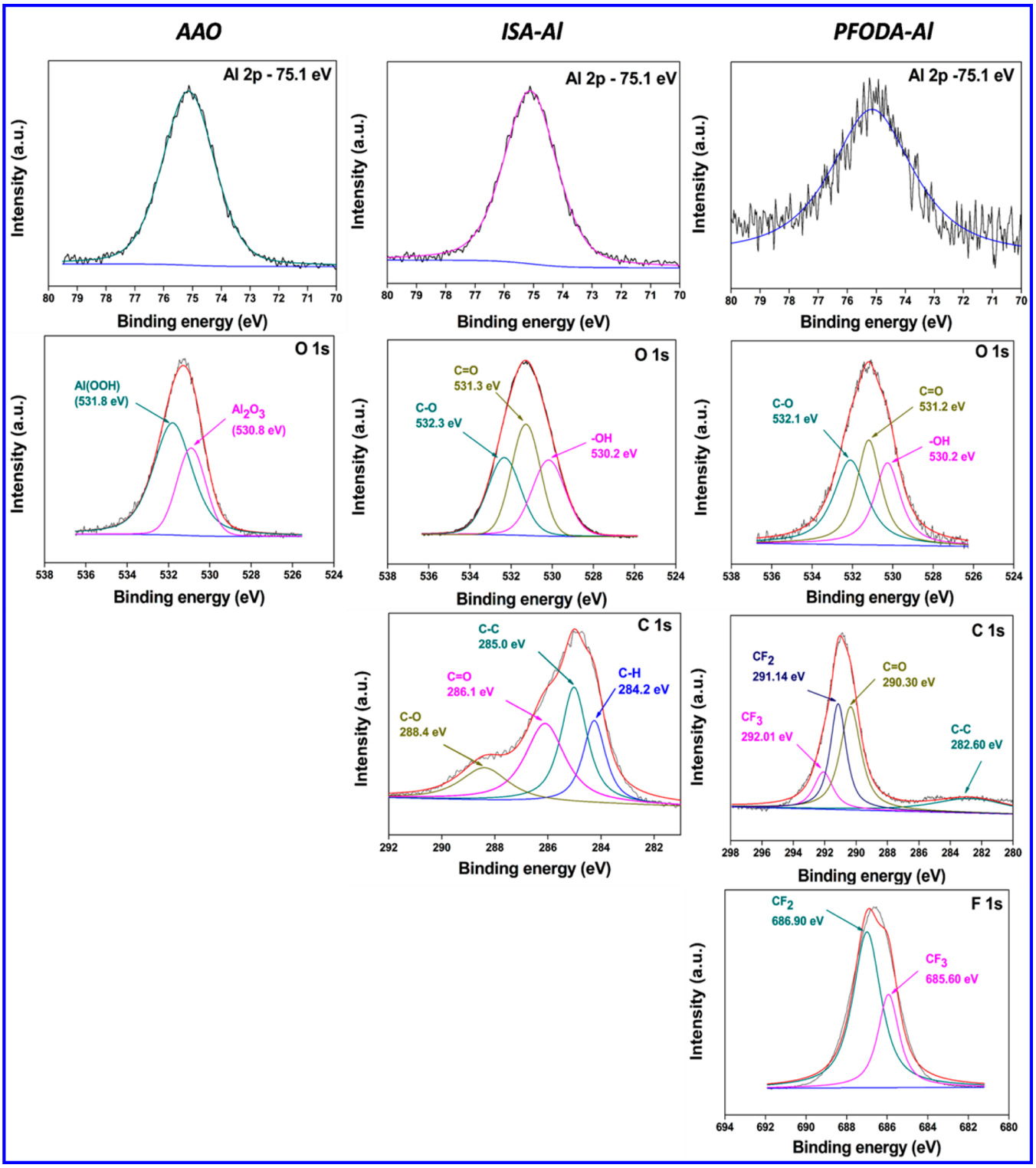

Figure 5. Deconvoluted XPS spectra of An-Al, ISA-Al, and PFODA-Al.

at 285 eV might originate from the C atoms belonging to the —C—C group. The third and fourth peaks at 286.1 and 288.4 eV are assigned to C═O and C—O from the carboxylate group formed on An-Al. Deconvoluted spectra of O 1s possess three peaks; —OH (530.2 eV), O═C (531.3 eV), —O—C (532.3 eV).

XPS deconvoluted spectra of PFODA-Al was also depicted in Figure 5, which shows elements such as Al, C, O, and F. As in the case of XPS spectra of ISA-Al, the peaks at 75 and 120.2 eV indicated the presence of Al 2p and Al 2s. Four peaks were fitted to the high-resolution spectra of C 1s; the peak at 282.6 eV corresponds to C—C, whereas the peak at 290.3 eV was attributed to the C atoms in C═O. The shift of 4.2 eV in C═O as compared to the binding energy of C═O (286.1 eV) in ISA-Al was noticed, which is due to the electronegativity of F atoms. The presence of CF_2 and CF_3 moieties was confirmed

DOI: 10.1021/am506568v
ACS Appl. Mater. Interfaces 2015, 7, 1516−1526

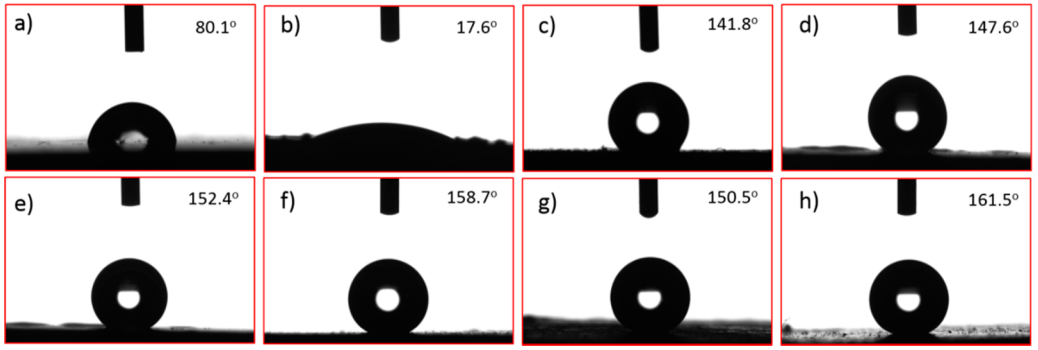

Figure 6. Water contact angle images of (a) bare, (b) An-Al, (c) DDA-Al, (d) TDA-Al, (e) ODA-Al, (f) ISA-Al, (g) PFSA-Al, and (h) PFODA-Al.

Table 1. Effect of Surface Free Energy and Roughness on Contact Angle[a]

sample	R_{rms} (nm)	contact angle (deg)		surface energy (mJ/m^2)			corrosion parameters		coefficient of friction
		water	1,2-DCE	γ^D	γ^P	γ^{tot}	I_{corr} (nA/cm^2)	E_{corr} (mV)	
bare	0.156	80.1	5.0	27.2	7.3	34.5	9097	−1135	0.471
An-Al	9.29	17.6	8.0	15.4	51.3	66.7	1090	−785	0.152
PFSA-Al	24.1	150.5	78.0	17.6	4.0	21.6	1050	−648	0.125
DDA-Al	10.8	141.8	67.0	21.7	2.9	24.6	719	−675	0.135
TDA-Al	13.8	147.6	72.0	19.9	3.5	23.4	528	−638	0.116
ODA-Al	15.3	152.4	81.0	15.8	3.2	19.0	369	−586	0.085
ISA-Al	25.0	158.7	96.0	9.7	2.3	12.0	49	−532	0.060
PFODA-Al	36.7	161.5	116.0	3.8	0.8	4.6	2.26	−328	0.045

[a]Corrosion and tribological parameters are also shown to elucidate corrosion protection and friction reducing behavior.

by the peaks at 291.1 and 292.0 eV, respectively. Three peaks were fitted to the high-resolution O 1s spectra; 530.2 eV (—OH), 531.2 eV (C═O) and 532.1 eV (—O—C). In addition to this peaks, a peak at 686 eV was observed, which indicates the existence of F atoms. Deconvoluted spectra of high resolution F 1s shows two peaks at 685.6 eV (CF_2) and 686.9 eV (CF_3). These values are being matched with the literature values.[37] The above results obtained from the EDX and XPS confirm the formation of carboxylate groups onto the as-formed AAO, which was well supported by the information provided by FTIR, SEM, FESEM, and AFM.

3.5. Surface Wettability. In an effort to describe the wettability of the modified surfaces, WCA measurements were carried out using a video based optical contact angle meter. Figure 6 shows the images of WCAs on the surface of the different types of Al substrates. The results obtained from the contact angle instrument are tabulated, which are presented as Table T1 (given in SI S8). SCA of bare Al was about 80.1°, which is slightly hydrophobic in nature. After being anodized using oxalic acid, SCA was reduced much to 17.6°, indicating near superhydrophilicity, probably due to the formation of active hydroxyl groups on the surface of Al observed by the EDX spectrum of the AAO surface. The transition from superhydrophilic to superhydrophobic behavior of Al occurred when anodized Al was covalently linked to low surface energy molecules. It is observed that as the number of alkyl chain in the modifier increases from 12 to 20 C, the WCA increases from 141.8° to 158.6° respectively. The higher SCA (161.5°) was achieved, as expected, in the case of the PFODA modified anodized Al surface, since the surface energy of the substrate was very low, compared to previously used fatty acids. Hence, it implies that the modifier obstructs the water molecules from penetrating into the base surface, helping the surface to be used with a self-cleaning property. Superhydrophobicity not only depends on high SCA, but also on low CAH. ACA and RCA were also investigated to explain wettability in terms of CAH. It is noted from SI Table T1 (given in SI S8) that the CAH was very low (2°) for PFODA-Al, 5° for ISA-Al and greater than 5° for all other fabricated samples.

3.6. Effect of Roughness and Surface Free Energy on Superhydrophobicity. In general, superhydrophobicity is believed to be related with two important parameters; hierarchical surface (high roughness) and low surface energy. The superhydrophobic behavior on modified Al surfaces is achieved due to the hierarchical roughness evidenced by surface morphological studies and low surface free energy calculated from the contact angle instrument (Table 1). Roughness plays a vital role in illustrating the superhydrophobic behavior.[55] The roughness parameters were obtained by the profile extraction of AFM topographic images, and the results are summarized in SI Table T2 (S9). The SCA changes of bare, anodized, and functionalized samples with the roughness could be well explained by these parameters. The R_{rms} roughness increases to render the substrates superhydrophobic, and maximum R_{rms} was observed for PFODA-Al (36.7 nm), which shows high WCA-161.5°, as expected.

It is necessary to elucidate the surface energy changes from untreated to treated samples, since it is demonstrated that the low surface energy was one of the main factors in determining the superhydrophobic behavior. Gawalt et al.[56] calculated the surface free energy of functionalized solid surfaces from the Young−Good−Girifalco−Fowkes equation as follows:

$$\gamma_{LV}(1 + \cos\theta) = 2(\gamma^{P}_{SV}\gamma^{P}_{LV})^{1/2} + 2(\gamma^{D}_{SV}\gamma^{D}_{LV})^{1/2} \quad (1)$$

where θ is the contact angle; γ_{LV}, γ^{P}_{LV}, γ^{D}_{LV} are the total, polar, and dispersive surface free energies of the liquid−vapor interface, respectively, and γ^{P}_{SV} and γ^{D}_{SV} are the polar and dispersive surface free energies of the solid−vapor interface. We

DOI: 10.1021/am506568v
ACS Appl. Mater. Interfaces 2015, 7, 1516−1526

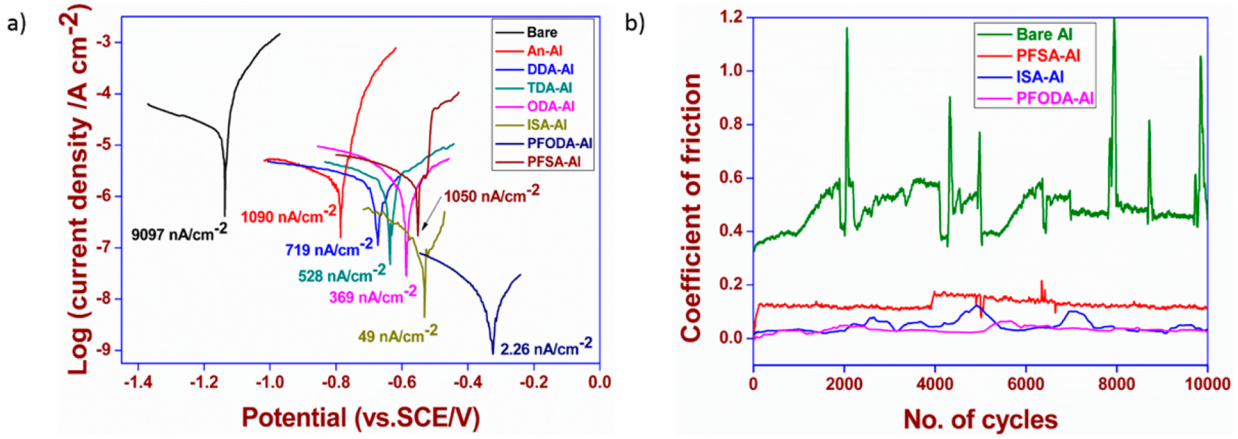

Figure 7. (a) Tafel plots of Bare, An-Al and chemically modified An-Al substrates immersed in 3.5 wt % NaCl solution. (b) CoF versus sliding cycles against steel disc obtained from pin-on-disc tribometer at a sliding velocity of 1 m/s.

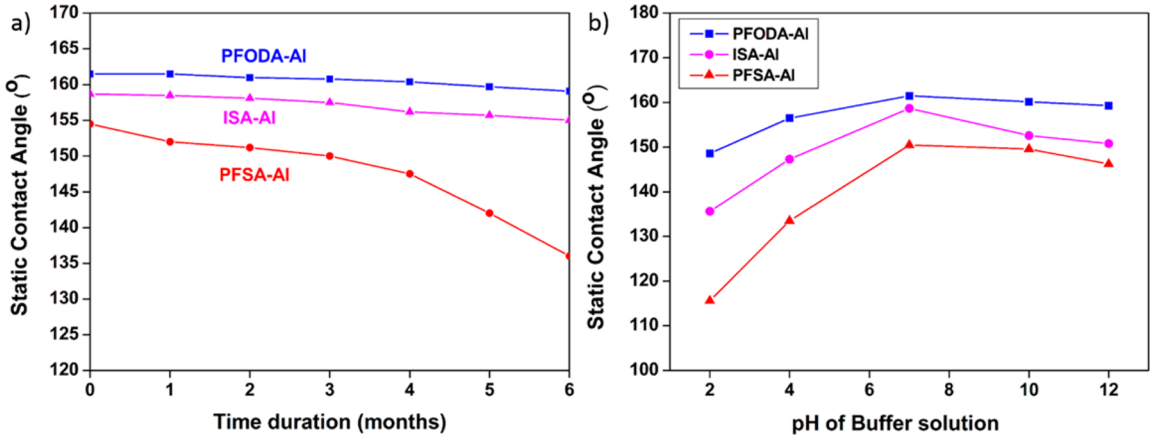

Figure 8. (a) Graph showing durability of PFODA-Al, ISA-Al, and PFSA-Al when exposed to air at ambient temperature. (b) Static Contact Angle of grafted samples soaked in buffer solutions of various pH for 30 min followed by being rinsed with water and dried at 110 °C.

also calculated the values of γ^{P}_{SV} and γ^{D}_{SV} using the same method with the help of the contact angle meter using water and 1,2-dichloroethane in which their surface free energies are known. The obtained values are displayed in Table 1. It is inferred that the low surface energy (4.6 mJ/m^2) obtained for PFODA coated Al was also responsible for its improved hydrophobicity. The surface free energies of ISA-Al and PFSA-Al were calculated to be 12.0 and 21.6 mJ/m^2, which also show superhydrophobic behavior.

3.7. Corrosion Resistive and Friction Reducing Properties. *3.7.1. Corrosion Resistive Behavior.* Instantaneous corrosion rate of substrates could be measured using polarization curves. From a typical polarization curve, it is possible to derive the important parameters, such as corrosion potential (E_{corr}) and corrosion current density (I_{corr}) in order to properly explain the mechanism of protection. In general, the lower I_{corr} value emphasize lower corrosion dynamic rate and positive E_{corr} value indicates lower corrosion thermodynamical tendency. Tafel plots were acquired to compare the corrosion behavior of bare, An-Al and fatty acids modified An-Al. We obtained potentiodynamic polarization curves after the stable open circuit potential was attained when the untreated and treated samples are exposed to 3.5 wt % NaCl solution at room temperature for 30 min. Figure 7a suggests that the anodized samples are having a low I_{corr} value and a high E_{corr} value as compared to bare, which indicates the resistivity to corrosion, mainly because of the protective oxide layer formed on the surface of Al. Further, it is also inferred from Figure 7a that the chemically modified samples with low surface energy molecules are showing better resistance to corrosion than An-Al, as indicated by the much lower I_{corr} and higher, positive E_{corr} values. This is probably due to the chemical interfacial force acting between the substrate and the low surface energy molecules. The result shows that a hydrophobically treated AAO surface significantly enhances the corrosion resistance compared to hydrophilic oxide surfaces. Interestingly, it is also observed that as the WCA increases for the substrates, the corrosion rate is found to decrease, which is due to the resistance toward water molecules around the surface (WCA increases from 141° to 161°). In order to further check the sustainability of the modification due to aging, the modified sample was left in the 3.5 wt % NaCl solution for a week and found the retention of superhydrophobicity with reference to the freshly modified samples.

3.7.2. Tribological Studies. The self-lubricating property of the fabricated Al was analyzed using tribological parameters such as wear rate and friction force. Generally, the friction-reducing behavior of modified substrates are expressed in terms of coefficient of friction (CoF) obtained from frictional force values. CoF values should be as low as the control samples in order to reduce friction.[57] In this manner, dry tribological studies at an applied load of 10 N were performed to evaluate

DOI: 10.1021/am506568v
ACS Appl. Mater. Interfaces 2015, 7, 1516−1526

the self-lubricative property of the modified substrates. The obtained CoF values were plotted against sliding cycles, which is depicted in Figure 7b. It is inferred that fatty acids modified An-Al exhibits very low and stable CoF ranging from 0.13 to 0.06 depending on the chemisorbed molecules as compared to bare (0.47) and An-Al (0.15). In specific, PFODA-Al shows a very low CoF value of about 0.05 exemplifying the higher lubricity and antiwear. This is mainly because of low surface energy as well as hierarchical nanostructure on the Al surface. The parameters obtained from the corrosion and wear tests are displayed in Table 1 along with WCA values. These findings will be of considerable importance in tribological applications.

3.8. Durability. As of today, the durability of the modified surfaces is a challenging area to work with, in terms of its industrial applications. Many research groups are working on this particular field to fabricate highly efficient and durable substrates.[42] In view of this, we attempted to evaluate the durability of the functionalized Al surfaces in different aspects: (a) exposed to air for 6 months at ambient temperature, (b) exposed at high temperature, (c) immersed in 3.5 wt % NaCl solution for a week, and (d) dipped in buffer solutions of various pH for 30 min and then checked their wettability. Figure 8a,b shows the plot of SCA against time duration in months and pH of buffer solutions used. These figures clearly demonstrate that the samples prepared under this technique are extremely stable and have a high degree of durability and repeatability.

4. CONCLUSIONS

A simple and adaptable solution immersion process (immersion time, 10 s) is reported to modify homogeneously ordered nanoporous AAO obtained by the electrochemical mild anodization of aluminum. The covalent linkages between the molecules and the substrate are the key factor for the preparation of stable and highly durable superhydrophobic hierarchical Al surface. These linkages are confirmed by FTIR-ATR and XPS analysis. The hierarchical roughness shown by the surface morphological techniques is also responsible for its superhydrophobicity apart from low surface energy. As compared to PFSA, PFODA-coated Al exhibits as high as 161.5° WCA and high resistivity toward corrosion because the fabricated surface can serve as a barrier layer to obstruct the diffusion of water, Cl^-, and O_2. Moreover, PFODA molecules possess very low surface energy and high lubricity. The corrosion rate (I_{corr}) was substantially reduced to 2.26 nA/cm^2 with E_{corr} value −328 mV vs SCE (after being modified with PFODA) when compared to bare (I_{corr}) 9.10 μA/cm^2 with an E_{corr} value of −1135 mV vs SCE. Compared with bare and AAO, the self-lubricated composites exhibited low frictional coefficient and longer wear life. Hence, the technique to create homogeneously ordered superhydrophobic nanosurface is projected as a long lasting, environmentally friendly, and highly efficient process adaptable for industry.

■ ASSOCIATED CONTENT

Supporting Information

Procedure for the formation of microvalleys, FTIR spectra of fatty acids, AFM images of saturated fatty acids coated anodized aluminum using oxalic acid, AFM images of microvalleys and PFODA-coated microvalleys, EDX spectra of anodized and modified samples, XPS survey scan spectrum of ISA-coated Al and PFODA-coated Al, and optical image showing super-hydrophobic behavior. This material is available free of charge via the Internet at http://pubs.acs.org.

■ AUTHOR INFORMATION

Corresponding Author

*Phone: +91-9443492420; E-mail: manbu123@gmail.com.

Notes

The authors declare no competing financial interest.

■ ACKNOWLEDGMENTS

This work is financially supported by the Department of Science and Technology (DST), New Delhi (GAP-08/13), and Council of Scientific and Industrial Research (CSIR), New Delhi (12 FYP-CSC-0114, INTELCOAT). The authors gratefully acknowledge the assistance of Dr. M. Duraiselvam and Mr. R. Ramesh, National Institute of Technology, Thiruchirappalli, India, during the tribological studies.

■ REFERENCES

(1) Li, F.; Zhang, L.; Metzger, R. M. On the Growth of Highly Ordered Pores in Anodized Aluminum Oxide. *Chem. Mater.* **1998**, *10*, 2470−2480.

(2) Dotzauer, D. M.; Dai, J.; Sun, L.; Bruening, M. L. Catalytic Membranes Prepared Using Layer-by-Layer Adsorption of Polyelectrolyte/metal Nanoparticle Films in Porous Supports. *Nano Lett.* **2006**, *6*, 2268−2272.

(3) Simovic, S.; Losic, D.; Vasilev, K. Controlled Drug Release from Porous Materials by Plasma Polymer Deposition. *Chem. Commun.* **2010**, *46*, 1317−1319.

(4) Aw, M. S.; Simovic, S.; Addai-Mensah, J.; Losic, D. Polymeric Micelles in Porous and Nanotubular Implants as a New System for Extended Delivery of Poorly Soluble Drugs. *J. Mater. Chem.* **2011**, *21*, 7082−7089.

(5) Alvarez, S. D.; Li, C.; Chiang, C. E.; Schuller, I. K.; Sailor, M. J. A Label-Free Porous Alumina Interferometric Immunosensor. *ACS Nano* **2009**, *3*, 3301−3307.

(6) Pan, S.; Rothberg, L. J. Interferometric Sensing of Biomolecular Binding Using Nanoporous Aluminum Oxide Templates. *Nano Lett.* **2003**, *3*, 811−814.

(7) Wang, M.; Meng, G.; Huang, Q.; Xu, Q.; Chu, Z.; Zhu, C. FITC-Modified PPy Nanotubes Embedded in Nanoporous AAO Membrane Can Detect Trace PCB20 via Fluorescence Ratiometric Measurement. *Chem. Commun.* **2011**, *47*, 3808−3810.

(8) Cheng, W.; Steinhart, M.; Gösele, U.; Wehrspohn, R. B. Tree-like Alumina Nanopores Generated in a Non-Steady-State Anodization. *J. Mater. Chem.* **2007**, *17*, 3493−3495.

(9) Zakeri, R.; Watts, C.; Wang, H.; Kohli, P. Synthesis and Characterization of Nonlinear Nanopores in Alumina Films. *Chem. Mater.* **2007**, *19*, 1954−1963.

(10) Liu, Y.; Goebl, J.; Yin, Y. Templated Synthesis of Nano-structured Materials. *Chem. Soc. Rev.* **2013**, *42*, 2610−2653.

(11) Yamaguchi, A.; Uejo, F.; Yoda, T.; Uchida, T.; Tanamura, Y.; Yamashita, T.; Teramae, N. Self-Assembly of a Silica-Surfactant Nanocomposite in a Porous Alumina Membrane. *Nat. Mater.* **2004**, *3*, 337−341.

(12) Smuleac, V.; Butterfield, D.; Sikdar, S.; Varma, R.; Bhattacharyya, D. Polythiol-Functionalized Alumina Membranes for Mercury Capture. *J. Membr. Sci.* **2005**, *251*, 169−178.

(13) Mutalib Md Jani, A.; Anglin, E. J.; McInnes, S. J. P.; Losic, D.; Shapter, J. G.; Voelcker, N. H. Nanoporous Anodic Aluminium Oxide Membranes with Layered Surface Chemistry. *Chem. Commun.* **2009**, 3062−3064.

(14) Gong, J.; Butler, W. H.; Zangari, G. Tailoring Morphology in Free-Standing Anodic Aluminium Oxide: Control of Barrier Layer Opening down to the Sub-10 nm Diameter. *Nanoscale* **2010**, *2*, 778−785.

DOI: 10.1021/am506568v
ACS Appl. Mater. Interfaces 2015, 7, 1516−1526

(15) Md Jani, A. M.; Losic, D.; Voelcker, N. H. Nanoporous Anodic Aluminium Oxide: Advances in Surface Engineering and Emerging Applications. *Prog. Mater. Sci.* **2013**, *58*, 636−704.
(16) Reis, F. D. A. A.; Badiali, J. P.; di Caprio, D. Modeling Growth of Organized Nanoporous Structures by Anodic Oxidation. *Langmuir* **2012**, *28*, 13034−13041.
(17) Cheng, C.; Ngan, A. H. W. Growth Sustainability of Nanopore Channels in Anodic Aluminum Oxide Guided with Prepatterns. *J. Phys. Chem. C* **2013**, *117*, 12183−12190.
(18) Darmanin, T.; Guittard, F. Recent Advances in the Potential Applications of Bioinspired Superhydrophobic Materials. *J. Mater. Chem. A* **2014**, *2*, 16319−16359.
(19) Liang, J.; Hu, Y.; Wu, Y.; Chen, H. Fabrication and Corrosion Resistance of Superhydrophobic Hydroxide Zinc Carbonate Film on Aluminum Substrates. *J. Nanomater.* **2013**, *2013*, 1−6.
(20) He, T.; Wang, Y.; Zhang, Y.; Lv, Q.; Xu, T.; Liu, T. Super-Hydrophobic Surface Treatment as Corrosion Protection for Aluminum in Seawater. *Corros. Sci.* **2009**, *51*, 1757−1761.
(21) Guo, X.; Xu, S.; Zhao, L.; Lu, W.; Zhang, F.; Evans, D. G.; Duan, X. One-Step Hydrothermal Crystallization of a Layered Double Hydroxide/Alumina Bilayer Film on Aluminum and Its Corrosion Resistance Properties. *Langmuir* **2009**, *25*, 9894−9897.
(22) Li, X.-M.; Reinhoudt, D.; Crego-Calama, M. What Do We Need for a Superhydrophobic Surface? A Review on the Recent Progress in the Preparation of Superhydrophobic Surfaces. *Chem. Soc. Rev.* **2007**, *36*, 1350−1368.
(23) Sun, T.; Feng, L.; Gao, X.; Jiang, L. Bioinspired Surfaces with Special Wettability. *Acc. Chem. Res.* **2005**, *38*, 644−652.
(24) Ruan, M.; Li, W.; Wang, B.; Deng, B.; Ma, F.; Yu, Z. Preparation and Anti-Icing Behavior of Superhydrophobic Surfaces on Aluminum Alloy Substrates. *Langmuir* **2013**, *29*, 8482−8491.
(25) Scardino, A.; De Nys, R.; Ison, O.; O'Connor, W.; Steinberg, P. Microtopography and Antifouling Properties of the Shell Surface of the Bivalve Molluscs *Mytilus galloprovincialis* and *Pinctada imbricata*. *Biofouling* **2003**, *19*, 221−230.
(26) Liu, T.; Yin, Y.; Chen, S.; Chang, X.; Cheng, S. Super-Hydrophobic Surfaces Improve Corrosion Resistance of Copper in Seawater. *Electrochim. Acta* **2007**, *52*, 3709−3713.
(27) Steinberger, A.; Cottin-Bizonne, C.; Kleimann, P.; Charlaix, E. High Friction on a Bubble Mattress. *Nat. Mater.* **2007**, *6*, 665−668.
(28) Kwon, G.; Kota, A. K.; Li, Y.; Sohani, A.; Mabry, J. M.; Tuteja, A. On-Demand Separation of Oil−Water Mixtures. *Adv. Mater.* **2012**, *24*, 3666−3671.
(29) Qian, B.; Shen, Z. Fabrication of Superhydrophobic Surfaces by Dislocation-Selective Chemical Etching on Aluminum, Copper, and Zinc Substrates. *Langmuir* **2005**, *21*, 9007−9009.
(30) Zheludkevich, M. L.; Salvado, I. M.; Ferreira, M. G. S. Sol−Gel Coatings for Corrosion Protection of Metals. *J. Mater. Chem.* **2005**, *15*, 5099−5111.
(31) Ma, W.; Wu, H.; Higaki, Y.; Otsuka, H.; Takahara, A. A "Non-Sticky" Superhydrophobic Surface Prepared by Self-Assembly of Fluoroalkyl Phosphonic Acid on a Hierarchically Micro/nano-structured Alumina Gel Film. *Chem. Commun.* **2012**, *48*, 6824−6826.
(32) Sas, I.; Gorga, R. E.; Joines, J. A.; Thoney, K. A. Literature Review on Superhydrophobic Self-Cleaning Surfaces Produced by Electrospinning. *J. Polym. Sci., Part B: Polym. Phys.* **2012**, *50*, 824−845.
(33) Xu, L.; Karunakaran, R. G.; Guo, J.; Yang, S. Transparent, Superhydrophobic Surfaces from One-Step Spin Coating of Hydrophobic Nanoparticles. *ACS Appl. Mater. Interfaces* **2012**, *4*, 1118−1125.
(34) Han, J. T.; Zheng, Y.; Cho, J. H.; Xu, X.; Cho, K. Stable Superhydrophobic Organic−Inorganic Hybrid Films by Electrostatic Self-Assembly. *J. Phys. Chem. B* **2005**, *109*, 20773−20778.
(35) Shi, F.; Wang, Z.; Zhang, X. Combining a Layer-by-Layer Assembling Technique with Electrochemical Deposition of Gold Aggregates to Mimic the Legs of Water Striders. *Adv. Mater.* **2005**, *17*, 1005−1009.
(36) Hosono, E.; Fujihara, S.; Honma, I.; Zhou, H. Superhydrophobic Perpendicular Nanopin Film by the Bottom-up Process. *J. Am. Chem. Soc.* **2005**, *127*, 13458−13459.
(37) Weibel, D. E.; Michels, A. F.; Feil, A. F.; Amaral, L.; Teixeira, S. R.; Horowitz, F. Adjustable Hydrophobicity of Al Substrates by Chemical Surface Functionalization of Nano/Microstructures. *J. Phys. Chem. C* **2010**, *114*, 13219−13225.
(38) Ou, J.; Hu, W.; Xue, M.; Wang, F.; Li, W. One-Step Solution Immersion Process to Fabricate Superhydrophobic Surfaces on Light Alloys. *ACS Appl. Mater. Interfaces* **2013**, *5*, 9867−9871.
(39) Barthwal, S.; Kim, Y. S.; Lim, S. Mechanically Robust Superamphiphobic Aluminum Surface with Nanopore Embedded Microtexture. *Langmuir* **2013**, *29*, 11966−11974.
(40) Ou, J.; Hu, W.; Xue, M.; Wang, F.; Li, W. Superhydrophobic Surfaces on Light Alloy Substrates Fabricated by a Versatile Process and Their Corrosion Protection. *ACS Appl. Mater. Interfaces* **2013**, *5*, 3101−3107.
(41) Liu, Y.; Liu, J.; Li, S.; Liu, J.; Han, Z.; Ren, L. Biomimetic Superhydrophobic Surface of High Adhesion Fabricated with Micro-nano Binary Structure on Aluminum Alloy. *ACS Appl. Mater. Interfaces* **2013**, *5*, 8907−8914.
(42) Peng, S.; Tian, D.; Yang, X.; Deng, W. Highly Efficient and Large-Scale Fabrication of Superhydrophobic Alumina Surface with Strong Stability Based on Self-Congregated Alumina Nanowires. *ACS Appl. Mater. Interfaces* **2014**, *6*, 4831−4841.
(43) Lim, M. S.; Feng, K.; Chen, X.; Wu, N.; Raman, A.; Nightingale, J.; Gawalt, E. S.; Korakakis, D.; Hornak, L. a; Timperman, A. T. Adsorption and Desorption of Stearic Acid Self-Assembled Monolayers on Aluminum Oxide. *Langmuir* **2007**, *23*, 2444−2452.
(44) Liascukiene, I.; Steffenhagen, M.; Asadauskas, S. J.; Lambert, J. F.; Landoulsi, J. Self-Assembly of Fatty Acids on Hydroxylated Al Surface and Effects of Their Stability on Wettability and Nanoscale Organization. *Langmuir* **2014**, *30*, 5797−5807.
(45) Feng, L.; Zhang, H.; Mao, P.; Wang, Y.; Ge, Y. Superhydrophobic Alumina Surface Based on Stearic Acid Modification. *Appl. Surf. Sci.* **2011**, *257*, 3959−3963.
(46) Saleema, N.; Sarkar, D. K.; Gallant, D.; Paynter, R. W.; Chen, X.-G. Chemical Nature of Superhydrophobic Aluminum Alloy Surfaces Produced via a One-Step Process Using Fluoroalkyl-Silane in a Base Medium. *ACS Appl. Mater. Interfaces* **2011**, *3*, 4775−4781.
(47) Buijnsters, J. G.; Zhong, R.; Tsyntsaru, N.; Celis, J.-P. Surface Wettability of Macroporous Anodized Aluminum Oxide. *ACS Appl. Mater. Interfaces* **2013**, *5*, 3224−3233.
(48) Grignard, B.; Vaillant, A.; de Coninck, J.; Piens, M.; Jonas, A. M.; Detrembleur, C.; Jerome, C. Electrospinning of a Functional Perfluorinated Block Copolymer as a Powerful Route for Imparting Superhydrophobicity and Corrosion Resistance to Aluminum Substrates. *Langmuir* **2011**, *27*, 335−342.
(49) Höhne, S.; Blank, C.; Mensch, A.; Thieme, M.; Frenzel, R.; Worch, H.; Müller, M.; Simon, F. Superhydrophobic Alumina Surfaces Based on Polymer-Stabilized Oxide Layers. *Macromol. Chem. Phys.* **2009**, *210*, 1263−1271.
(50) Tan, T. T. Y.; Ahsan, A.; Reithofer, M. R.; Tay, S. W.; Tan, S. Y.; Hor, T. S. A.; Chin, J. M.; Chew, B. K. J.; Wang, X. Photoresponsive Liquid Marbles and Dry Water. *Langmuir* **2014**, *30*, 3448−3454.
(51) Mo, Y.; Bai, M. Preparation and Adhesion of a Dual-Component Self-Assembled Dual-Layer Film on Silicon by a Dip-Coating Nanoparticles Method. *J. Phys. Chem. C* **2008**, *112*, 11257−11264.
(52) Zhang, Q.; Wan, Y.; Li, Y.; Yang, S.; Yao, W. Friction Reducing Behavior of Stearic Acid Film on a Textured Aluminum Substrate. *Appl. Surf. Sci.* **2013**, *280*, 545−549.
(53) Zang, D.; Zhu, R.; Zhang, W.; Wu, J.; Yu, X.; Zhang, Y. Stearic Acid Modified Aluminum Surfaces with Controlled Wetting Properties and Corrosion Resistance. *Corros. Sci.* **2014**, *83*, 86−93.
(54) Ma, D.; Li, S.; Liang, C. Electropolishing of High-Purity Aluminium in Perchloric Acid and Ethanol Solutions. *Corros. Sci.* **2009**, *51*, 713−718.
(55) Mammen, L.; Deng, X.; Untch, M.; Vijayshankar, D.; Papadopoulos, P.; Berger, R.; Riccardi, E.; Leroy, F.; Vollmer, D. Effect of Nanoroughness on Highly Hydrophobic and Superhydrophobic Coatings. *Langmuir* **2012**, *28*, 15005−15014.

DOI: 10.1021/am506568v
ACS Appl. Mater. Interfaces 2015, 7, 1516−1526

(56) Kruszewski, K. M.; Gawalt, E. S. Perfluorocarbon Thin Films and Polymer Brushes on Stainless Steel 316 L for the Control of Interfacial Properties. *Langmuir* **2011**, *27*, 8120−8125.
(57) Li, P.; Chen, X.; Yang, G.; Yu, L.; Zhang, P. Fabrication and Characterization of Stable Superhydrophobic Surface with Good Friction-Reducing Performance on Al Foil. *Appl. Surf. Sci.* **2014**, *300*, 184−190.

DOI: 10.1021/am506568v
ACS Appl. Mater. Interfaces 2015, 7, 1516−1526